Profiling rare earth elements in Power River Basin sub-bituminous coal ash using laser-induced breakdown spectroscopy (LIBS)

Tran X. Phuoc, Ping Wang, and Dustin McIntyre

National Energy Technology Laboratory, Department of Energy, P. O. Box 10940, MS 84-340, Pittsburgh, PA 15261

CONFERENCE: 2015 World of Coal Ash – (www.worldofcoalash.org)

KEYWORDS: Rare earth elements, LIBS, coal, ash

ABSTRACT

Although coal ash has been identified as a potential source for rare earth production, it still remains as an untapped resource. This is because data on concentrations of trace rare earth elements in various coal ash wastes are not available. We will report here, therefore, our results on the use of laser-induced breakdown spectroscopy to analyze the rare earth elements contained in ash samples from Power River Basin sub-bituminous coal (PRB-coal). The pulse intensity of about 14.5 GW/cm^2 was used. Emission lines from the laser spark was analyzed using a spectrometer that can record a spectrum across the 200-980 nm range at a resolution of ~0.1 nm (FWHM). Ash was prepared by drying and burning PRB-coal powder of about 150 μm in a TGA at 750 ^{o}C. until the weight of the remaining ash became unchanged. The ash samples for LIBS experiments were made in the form of pellets by compressing about 1.5 grams of ash in a pellet die with a pressure of 15000 psi for 5 minutes. We have identified many elements in the Lanthanide series (cerium, europium, holmium, lanthanum, lutetium, praseodymium, promethium, samarium, terbium, ytterbium) and some elements in the actinide series (actinium, thorium, uranium, plutonium, berkelium, californium) in the ash samples. In addition, various metals were also seen to present in the ash samples. Procedures for quantifying their concentrations were briefly presented

INTRODUCTION

Rare earth elements are the chemical elements that are grouped in two series: the Lanthanide series (lanthanum, cerium, praseodymium, neodymium, promethium, samarium, europium, gadolinium, terbium, dysprosium, holmium, erbium, thulium, ytterbium, lutetium) and the Actinide series (Actinium, Thorium, Protactinium, Uranium, Neptunium, Plutonium, Americium Curium, Berkelium, Californium, Einsteinium, Fermium, Fm, Mendelevium, Nobelium, Lawrencium). Due to their unique magnetic, phosphorescent, and catalytic properties, these elements are the critical and irreplaceable materials in modern technologies (TVs, cellular phones, computers,

permanent magnet motors for wind turbines and disk drives, hybrid car batteries, compact fluorescent lighting, catalysts for refining heavier crude oil, automobile catalytic converters, etc.).

Traditionally, rare-earth elements are extracted mainly from natural mineral deposits. Recently, it has been reported that many rare earth elements were found in coal samples from certain regions in Germany and in the United Sates [1-5] in Bulgaria [6], and in Bangladesh [7]. Since the combustion of coal for energy generation results in highly concentrated non-volatile minerals in the coal ash wastes, the concentrations of rare-earth elements in coal ash could be enriched up to within the range of mineral ore deposits [8].

In our present work, various elements in ash samples from Power River Basin sub-bituminous coal will be qualitatively characterized using the LIBS technique. Many techniques such as X-ray fluorescence (XRF) [4], inductively coupled plasma–mass spectrometry (ICP-MS) [4], and neutron activation [6] have been used for coal and coal ash elemental composition analysis. As pointed out by Haider et al [7] and Yao et al. [9] the XRF method cannot detect lighter elements and the depth information is limited to only 1 – 2 μm. The neutron activation method, because it requires a strong radioactive/neutron source, is bulky and presents potential health hazards. Comparing with the above methods, LIBS does not have the limitations mentioned above. This is a fast, simple, reagent-free, and low-ppm level detection technique for many different situations [7, 9-13].

EXPERIMENT

The proximate, ultimate and ash mineral analysis of the sub-bituminous coal from Power River Basin are summarized in Table 1. Small coal pellets of 10 mm in diameter and about 2.5 mm thick were made for our LIBS measurements. To do so, we first ground the supplied coal powder and shook it through a 150 μm sieving machine. Each pellet was made by pouring about 1.5 g of the prepared powder into a pellet die and compressed with a pressure of 15000 psi for 5 minutes. Ash samples were prepared by drying, devolatilizing and burning the prepared coal powders in a TGA (Leco TGA-601). The drying and devolatilization processes were carried out under N_2 atmosphere at 107 ^oC and 950 ^oC, respectively. The devolatilized samples were cooled to 600 ^oC then burned at 750^oC under air environment until the weight of the remaining ash became unchanged. Ash pellets were prepared using the same procedure described above.

Table 1 Summary of chemical properties of Power River Basin sub-bituminous coal (PRB)

Proximate analysis (% dry basis)			Ultimate analysis (% dry basis)				
Volatile matter	Fixed carbon	ash	C	H	N	S	O
46.18	47.22	6.6 6	6.21	4.20	1.21	0.48	21.30

Ash mineral analysis (% wt)

SiO_2	Al_2O_3	Fe_2O_3	TiO_2	CaO	P_2O_5	MgO	Na_2O	K_2O	SO_3
38.71	16.00	5.52	1.08	19.24	0.96	4.68	1.22	0.75	10.99

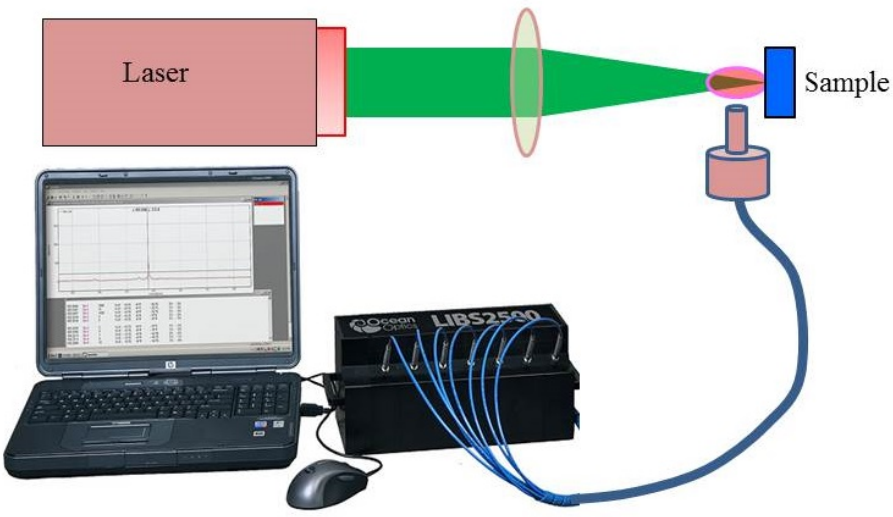

Figure 1. Schematic set up of the LIBS for REE profiling

The LIBS apparatus is schematically shown in Fig. 1. The apparatus consists mainly of a laser system, a spectrometer unit, a beam-delivery optics, and a sample holder. The laser system uses a single-mode, Q-switched Nd-Yag laser that is able to produce a laser pulse up to 100 mJ either at 1064 nm or 532 nm with a pulse duration of 5.5 ns and it delivered to the sample using a 75 mm focal length lens. The spectrometer (OceanOptics, LIBS2500) permits real-time, qualitative measurements of elements in solids. It provides spectral analysis across the 200-980 nm range at a resolution of ~0.1 nm (FWHM). During each experiment, LIBS sample was glued on the sample holder which was mounted on xyz translator so that it can be manually and continuously moved around the focal point. In our experiment, laser pulse energy of 25 mJ was focused onto the sample to create a spot size of about 200 μm using a 100 mm focal lens. The laser intensity was approximated to be about 14.5 GW/cm^2 at the spot. A delay of 1.5 μs between the firing of the laser and the acquisition of the LIBS spectra was applied. In order to reduce errors due to laser fluctuation and sample heterogeneity, a total of about 3 ash pellets and 3 coal pellets were tested and, for each

pellet, we created about 10 spectra. Thus, for each spectrum presented in the next section, the intensity of each emission line is the average value over about 30 of those measured by the present study.

RESULTS AND DISCUSSIONS

Figure 2 shows a typical LIBS spectrum spreading from 200 to 900 nm for coal and coal ash obtained by our present experiments. It is clear that, for all of these elements, their emission lines were more significantly pronounced and many of them became saturated in the ash samples than in the coal samples.

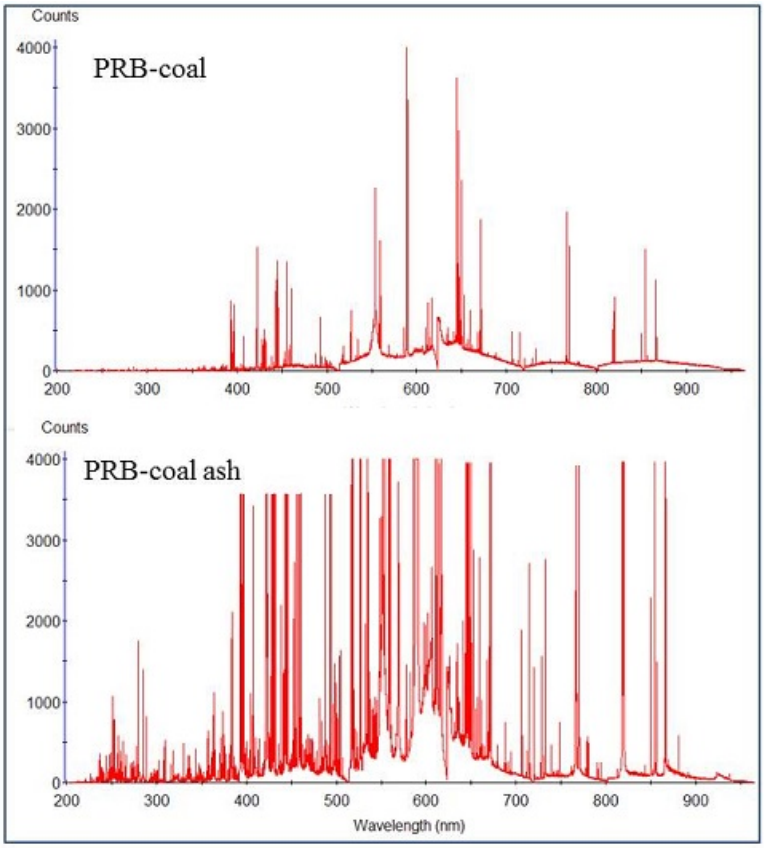

Figure 2. Typical LIBS spectrum observed for PRB-coal and PRB-coal ash

By comparing the wavelengths of the emission lines observed with those from the online NIST Atomic Spectra Database, we obtained a spectrum of numerous strong emission lines emitted by both neutral and single-ionized states of the various metals and rare earth elements in the lanthanide and actinide series present in our PRB-coal and coal ash samples. Because many of the emission lines from an element interfered significantly with those from others, in our present experiments, an element was considered to be identified if it had three or more emission lines that were unambiguous and did not interfere with those from other elements.

Table 3. Summary of the rare-earth elements identified in PRB-coal ash

Element	Unambiguous line detected, (wavelength in nm)	# of lines Detected
Lanthanide Series		
Cerium , Ce	522.346(I), 524.592(I), 571.903(I), 413.765(II), 456.236(II)	5/16
Europium, Eu	462.722(I), 583.098(I), 272.778(II), 368.842(II), 372.494(II), 412.970(II), 452.257(II)	7/22
Holmium, Ho	410.862(I), 412.716(I), 598.285(I), 341.644(II)	4/26
Lanthanum, La	514.542(I), 550.134 (I), 624.993 (I), 639.423(I), 379.478(II)	5/27
Lutetium, Lu	308.147(I), 337.65(I), 364.777(I), 412.473(I), 451.857(I), 600.452(I)	6/31
Praseodymium, Pr	395.944(I), 463.955(I), 501.976(I)	3/23
Promethium,Pm	475.9(I), 489.252(I), 652.045(I), 554.608(II), 557.602(II)	5/33
Samarium, Sm	447.089(I), 476.027(I), 484.17(I), 392.24(II)	4/33
Terbium, Tb	431.885(I), 464.531(I), 475.253(II)	3/28
Ytterbium, Yb	555.647(I), 679.96(I), 275.048(II), 297.056(II)	4/20
Actinide Series		
Actinium, Ac	635.986(I), 356.559(II), 450.720(II)	3/20
Thorium, Th	616.982(I), 411.671(II), 439.111(II)	3/31
Uranium, U	348.937(I), 381.199(I), 386.592(II), 454.363(II)	4/30
Plutonium, Pu	387.854(I), 863.019(I), 297.25(II), 333.771(II)	4/31
Berkelium, Bk	344.266(I), 565.903(I), 341.213(II), 419.744(II)	4/23
Californium, Cf	540.888(I), 372.211(II), 399.357(II)	3/17

Table 4. Summary of non- metal and metal elements present in PRB-coal ash samples

Element	Unambiguous line detected, (wavelength in nm)	# of lines Detected
S	542.867(II), 543.282(II), 545.563.997(II), 831.459(II)	4/29
Co	240.726(I), 241.162(I), 252.137(I)	3/24
Fe	248.327(I), 240.489(II), 258.588(II), 261.187(II), 273.955(II)	5/31
Ti	365.35(I), 395.633(I), 498.173(I), 499.107(I), 506.465(I), 323.451(II)	6/31
V	385.585(I), 437.923(I), 439.522(I), 440.819(I), 440.85(I), 609.021(I), 268.795(II)	7/31
W	255.135(I), 272.435(I), 429.461(I)	3/29
Zr	471.007(I), 355.659(II), 357.685(II)	3/31
Bi	293.83(I), 298.902(I), 306.77(I)	3/32
Te	400.652(II), 465.437(II), 564.926(II)	3/23
Be	457.266(I), 825.407(I), 467.333(II),	3/22
Mg	277.983(I), 516.732(I), 518.36(I), 279.078(II), 448.113(II), 448.133(II)	6/23
Ca	649.378(I), 657.278(I), 854.209(II), 866.214(II)	4/24
Sr	487.249(I), 496.226(I), 496.794(I), 525.69(I), 548.084(I), 640.847(I), 679.105(I), 687.838(I), 707.01/(I)	9/21
Ba	652.731(I), 659.533(I), 669.384(I), 705.994(I), 767.209(I), 856.743(I), 614.171(II)	14/22
Li	812.623(I), 812.645(I), 548.45(II), 548.511(II)	4/16
Cs	I852.113(I), 876.141(I), 894.347(I), 452.674(II)	4/17

With the identification criterion described above, elements that were identified with 3 or more unambiguous emission lines are tabulated in the following Tables 3 and 4. Other rare earth elements such as Dy, Er, Gd, Nd, Tm, Pa, Am, Cm, Es and numerous metal

elements (Ag, Au, Al, Cr, Ga, Ge, Hf, Hg, Mn, Mo, Na, Nb, Os, Pb, Pt, Ra, Rb, Ru, Sc, Si, Sn, Ta, Tc, Zn, Y) were also detected but were not included in these tables simply because the number of the unambiguous detected emission lines for these elements did not meet the identification criterion. We, however, did not detect Cd, Cu, Ni, Pd, Rh and the remaining elements of the actinide series (Neptunium, fermium, mendelevium, nobelium, lawrencium). This might be possible that our ash samples contain these elements at the concentration levels that our present experiment could not detect.

Under plasma conditions, all elements are ionized. If $N^{i}_{m,o}$ (particle/m^3) is the number density of the atoms of element i that are at charge state m and are on the ground level, (m = I for neutral, m = II for single-ionized) and if the laser-induced spark is assumed to be in local thermal equilibrium (LTE), the Boltzmann distribution can be used to calculate the population of such charged atoms on the kth level as:

$$N^{i}_{m,k} = N^{i}_{m,o} \frac{g^{i}_{m,k}}{Z^{i}_{m}} \exp\left(-\frac{E^{i}_{m,k}}{k_B T}\right) \tag{1}$$

Where $g^{i}_{m,k}$ is the kth level statistical weight, Z^{i}_{m} is the partition function, $E^{i}_{m,k}$ is the excitation energy of the kth level, k_B is the Boltzmann constant, and T is the absolute temperature. The absolute intensity of line emission is proportional to the population of the excited state. If the laser-induced spark in our experiments is assumed to be optically thin to avoid self-absorption, it is given as

$$I^{i}_{m} \propto A^{i}_{m,k} N^{i}_{m,k} h\nu_k \tag{2}$$

Where I^{i}_{m}, expressed in J/m^3-s, is the line intensity of the emission line emitted by the m-charged atoms of element i, h is the Plank's constant and $\nu_k = c/\lambda_k$ with λ_k is the wavelength of the transition from the excited state k and c is the speed of light. In actual measurements, the efficiency of the detection system affects the measured intensity of the line. Thus, by including a factor F representing such effect and replacing $\nu_k = c/\lambda_k$, we can approximate the emission intensity given by (2) as

$$I^{i}_{m} = \frac{F g^{i}_{m,k} N^{i}_{m,o} A^{i}_{m,k} hc}{Z^{I}_{i} \lambda_k} \exp\left(-\frac{E^{i}_{m,k}}{k_B T}\right) \tag{3}$$

Or

$$\mathrm{Ln}\left(\frac{I^{i}_{m} \lambda_k}{g^{i}_{m,k} A^{i}_{m,k} hc}\right) = \mathrm{Ln}\left(\frac{F N^{i}_{m,o}}{Z^{i}_{m}}\right) - \left(\frac{1}{T}\right)\frac{E^{i}_{m,k}}{k_B} \tag{4}$$

Where $A^{i}_{m,k}$ is the transition probability for the given emission line. Equation (4) represents the well-known Boltzmann plot and it indicates that, for a given temperature, the logarithmic values of the intensity of a emission line from an element calculated as

$\ln\left(I^i_m \lambda_k / g^i_{m,k} A^i_{m,k} hc\right)$ decreases linearly as its line energy increases. The slope of such a linear straight line is related to the emitting atom temperature and the intercept contains the information on the concentration of the charged atoms on the ground level. Thus, if the laser-induced spark plasma created from a sample containing multiple elements, since the temperature for all emitting atoms are the same in the LTE model, equation (4) will yield a series of parallel straight lines that can be used to quantify the plasma temperature and its element concentrations.

As an example, we show in Fig. 3 the Boltzmann plots of some elements identified in our ash samples (Eu II, V I, and W I). The calculations were carried out using the transition probability and other spectroscopic data tabulated in Table 5. It is clear that, for each element, values of $\mathrm{Ln}\left(I^i_I \lambda_k / g^i_{I,k} A^i_{I,k} hc\right)$ fluctuated around a straight line that was parallel with one another as functionally described by equation (4). The fluctuations here can be attributed to the random nature of the LIBS technique and also to the uncertainties in the existing literature on the transition probability A_k and other spectroscopic data. The results shown here also indicated that the plasma produced under our experiment conditions was close to LTE condition that was used to develop the above equations. We calculated the slopes of the lines to obtain an average plasma temperature of about 6575 K which is much lower than the range reported by Haider et al [7]. This might be due to difference in the power density used in our present experiment (14.5 GW/cm^2) compared to that (16 GW/cm^2) used by Haider et al. From the intercepts of the straight lines, we can also qualitatively conclude that, the concentrations of the four elements shown in Fig. 3, the concentration of tungsten was the most and it was followed by those of europium, and vanadium.

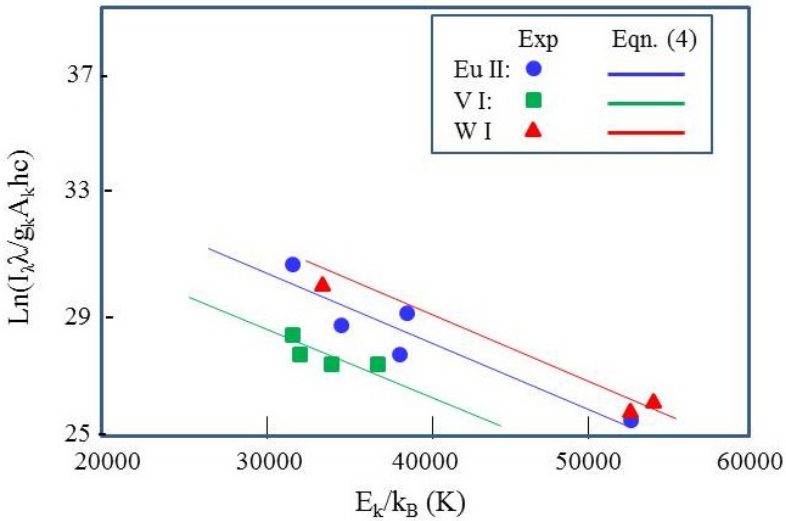

Figure 3. A typical Boltzmann plot showing the relationship between the detected line intensity with its line energy for some elements found in PRB-coal ash sample

Table 5. Summary of the transition probability and other spectroscopic data

	Observed		NIST database	
Element	Wavelength (nm)	Count	$g_{i,k}A_{i,k}$ (1/s)	E_k (1/cm)
Europium (Eu II)	272.778	57.000	7.20e+08	36648.95
	368.842	402.00	9.10e+07	27104.07
	372.494	166.00	4.00e+08	26838.50
	412.970	422.00	6.10e+08	24207.86
	452.257	603.00	6.90e+07	22105.07
Vanadian (V I)	385.585	186.00	4.68e+08	25927.33
	437.923	278.00	1.30e+09	22828.65
	439.522	186.00	3.30e+08	22745.56
	440.819	290.00	3.60e+08	22678.66
Tungsten (W I)	255.135	116.00	5.34e+8	39183.20
	272.435	106.00	7.35e+8	36695.12
	429.461	339.00	6.20e+7	23278.48

Although quantifying the concentrations of the detected elements is not our objective at present, procedures for doing just that is presented as follows. Let b_m^i be the intercept of each straight line in Fig. 3, for an element i, the density of its charged atoms on the ground level can be deduced as

$$N_{m,o}^{i} = \frac{Z_m^i e^{b_m^i}}{F} \tag{5}$$

If we assume that the emission lines from and element contains the mission lines from its neutral and single-ionized atoms only, the total number of the atoms of element i is calculated as

$$N_i = N_{I,o}^i + N_{II,o}^i = \frac{Z_I^i e^{b_I^i} + Z_{II}^i e^{b_{II}^i}}{F} \tag{6}$$

The relative concentration of an element is obtained as

$$X_i = \frac{N_i}{\sum_{\text{all elements}} N_i} = \frac{Z_I^i e^{b_I^i} + Z_{II}^i e^{b_{II}^i}}{\sum_{\text{all elements}} \left(Z_I^i e^{b_I^i} + Z_{II}^i e^{b_{II}^i} \right)} \tag{7}$$

As discussed by Ciucci et al [14] use of equation (7), concentrations of the elements content in a sample can be quantitatively determined without the need for system calibration. However, in order to use equation (7), it is required that the plasma spectrum must have all the emission lines by all the elements of the sample. Since F represents the detection efficiency of the detection system, it is necessary to keep F constant, thus, experimental parameters (number of laser shots, focal point, laser

intensity, light collecting optics, etc.) must be the same during the whole experiments. Spectroscopic data for all emitting species must be available and reliable so that their Boltzmann plots could be created. The first requirement is fulfilled because the spectrometer used by our present experiments permits a sensitive detection of a spectrum from 200 to 900 nm range, which is typically required to record all the emission lines by the elements in coal and ash samples. The last requirement, however, is difficult to fulfill at present due to the scarcity of the spectroscopic data. We, therefore, report here only the various elements that were identified from PRB sub-bituminous ash samples, work on quantifying their concentrations is continued and the results will be reported in due course.

CONCLUSIONS

We have conducted a simple LIBS experiment for identifying various metal and rare earth elements in PRB-coal ash samples. Our preliminary results indicated that PRB-coal ash contains a number of rare earth elements in both the Lanthanide series and the Actinide series. Various metal elements were also detected. Although, quantifying the concentrations of the detected elements is not our objective at present, some important steps for such purpose have been presented.

Disclaimer:

"This report was prepared as an account of work sponsored by an agency of the United States Government. Neither the United States Government nor any agency thereof, nor any of their employees, makes any warranty, express or implied, or assumes any legal liability or responsibility for the accuracy, completeness, or usefulness of any information, apparatus, product, or process disclosed, or represents that its use would not infringe privately owned rights. Reference herein to any specific commercial product, process, or service by trade name, trademark, manufacturer, or otherwise does not necessarily constitute or imply its endorsement, recommendation, or favoring by the United States Government or any agency thereof. The views and opinions of authors expressed herein do not necessarily state or reflect those of the United States Government or any agency thereof."

REFERENCES

[1] Seredin, V.V., and Dai S. International Journal of Coal Geology, 2012, 94, p.67.

[2] Coles, D.G., Ragaini, .RC., and Ondov,J.M., Am. Chem. Soc, 1979, 13, p.455.

[3] Izquierdo, M., and Querol, X., International Journal of Coal Geology, 2012, 94, p.54

[4] Zhang, Y., Talbott, J.L., Wiedenmann, L., DeBarr, J., and Demir, I., Proceedings of the Denver X-ray Conference, Advances in X-ray Analysis, 1997, 94, p.879.

[5] Arrioyo, F., Font, O., Fernandez-Pereira, C., Querol, X., Chimenos, J.P., and Zeegers, H., World of Coal Ash Conference, 2009, available at www.flyash.inf].

[6] Eskenazy, G.M. International Journal of Coal Geology, 1987, 7, p.301

[7] Haider AFMY. Rony, MA. Lubna, RS. And Abedin, KM., Optics & Laser Technology, 2011, 43, p1405.

[8] Mayfield, D.B, and Lewis, A.S., 2013 World of Coal Ash (WOCA) Conference, April 22-25, 2013, Lexington, KY (http://www.flyash.info].

[9] Shunchun Yao, Jidong Lu, Meirong Dong, Kai Chen, Junyan Li, and Jun Li., Applied Spectroscopy, 2011, 65, p.1197.

[10] Jie Li, Jidong Lu, Zhaoxiang Lin, Shunsheng Gong, Chengli Xie, Liang Chang, Lifei Yang, and Pengyan Li, Optics&LaserTechnology, 2009, 41, p.907.

[11] Wangbao Yin, Lei Zhang, Lei Dong, Weiguang Ma, and Suotang Jia, Applied Spectroscopy 2009, 63, p. 865.

[12] Alice Stankova, Nicole Gilon, Lionel Dutruch, Viktor Kanicky, Fuel, 2010, 89, p.3468.

[13] T. Ctvrtnickov , M.P. Mateo, A. Yañez, G. Nicolas, Spectrochimica Acta Part B, 2010, 65, p. 734.

[14] Ciucci, A., Corsi, M., Palleschi, V., Rastelli, S., Salvetti, A., and Tognoni, E., Applied Spectroscopy, 1999, 53, p.960